bioresources.com

Advances on Geometrical Limits in the Deep Drawing Process of Paperboard

Marek Hauptmann,* Sebastian Kaulfürst, and Jens-Peter Majschak

The geometrical limits of the deep drawing process of paper to advanced shapes are not known. This report examines the technological limits of convex elements of the base shape in relation to the drawing height and shows the material behavior in the bottom radius of 3D shapes with regard to special material properties. In the bottom radius, non-compressed wrinkles occurred due to the in-plane compression, but wrinkles were reduced by an increased blank holder force or tool temperatures and improved extensibility or in-plane compressive strain. The forming ratio during deep drawing (drawing height related to base diameter) was increased to a value of more than 1 by a blank holder force, which increased with the drawing height such that the initial blank holder force was reduced concurrently. Straight sections in the base shape reduced the risk for ruptures in the edge radii of rectangular shapes, producing a forming ratio in these radii of 2.5. The forming ratio was further supported by a pattern of creasing lines at the blanks with a radial orientation and a number near the expected maximum number of wrinkles. The spring-back at rectangular shapes mainly depended on the drawing height and edge radius.

INTRODUCTION

Paperboard is one of the most commonly used packaging materials in the world and experiences broad acceptance due to its end of life options including biodegradation and recyclability. However, in advanced packaging applications with high demands on visual quality, rigidity, resistance against migration, and permeation of oligomers or gases, the material has shortcomings. These disadvantages result from the forming behavior of the material. There has been a widespread expectation that packaging containers prepared from 3D-formed paperboard would not be able to compete at the point of sale.

Recent developments in 3D-forming technologies and the ongoing search for more sustainable packaging solutions have created increasing interest in paperboard and primary packaging. However, the forming limits with the current state of 3D-forming technologies have not been fully exploited. Currently, there are three approaches for the 3D-forming of paperboard. The hydroforming technology forms the paperboard with a rubber membrane in a female mould (Mozetic 2008). The usual objective of this technological approach is to stretch the material to its maximum without overloading the most intensely strained sections to avoid the appearance of wrinkles. The limitations of geometrical features have not been described in detail, but the forming ratio (with forming height in comparison to

the base diameter or base dimensions) can be estimated by the test geometries (Groche and Huttel 2016), which reach a forming ratio of approximately 0.11 with a double-curved mould. Östlund *et al*. (2011) also used a double curved mould, producing a forming ratio of 0.15. Special laboratory materials engineered for increased extensibility improved these forming ratios significantly. The highest extensibility was reported by Vishtal and Retulainen (2014), who used agar as a wet web preparation agent and achieved a strain of nearly 30%. With this strain, a forming ratio of approximately 0.4 was demonstrated without wrinkles in a fixed blank forming process. With a sliding blank, the forming ratio with this type of material was increased to approximately 0.7.

Pressmolding is typically performed with forming ratios in the range of 0.3 to 0.4 using commercial board grades (Tanninen *et al.* 2015). This process works with mechanical tools. A male mold presses the material into a female mold, while a blank holder applies a controlled force without fixing the material completely. The forming is supported by a creasing line pattern on the blank, and wrinkles occur. Typical tray radii on the edges of rectangular base geometries range from 30 to 80 mm. The shapes are often combined with a rounding radius from the bottom to the wall of the cup of approximately 20 to 30 mm, during which the wrinkles are also present. Special materials improve the forming degree in pressforming, but there has been no publication systematically describing the geometrical limitations of this process.

Deep drawing of paperboard with immediate compression is the third 3D-forming approach. Its major difference from pressmolding is that the material is immediately compressed and densified in the cavity after passing the infeed radius, which enables an increased influence on the distribution of wrinkles; this results in a very fine and uniform arrangement of wrinkles over the wall without creasing the line pattern at the blank (Hauptmann and Majschak 2011). The maximum forming ratio was 0.63, and rectangular shapes with an edge radius of 15 mm and a size of 90x90 mm were successfully deep drawn to a height of 25 mm (Hauptmann and Majschak 2012). Furthermore, Hauptmann *et al.* (2014) produced concave elements in the base shape. A concave depth of 3 mm was drawn with a commercial board grade (6% strain at break) to a height of 15 mm at 38 mm concave radius. These parameters lead to a needed strain of 28% at 15 mm drawing height. Material qualities with improved strain at break lead to further improved limits. An improved strain at break might also improve the limitations in forming ratio because the strain of the wall contributes to the final height of the 3D shape. The limitations in forming ratio in combination with rectangular shapes and their edge radii still need more data to better describe the capabilities of the forming process deep-drawing with immediate compression. There is also relatively little data concerning the application of an edge radius between bottom and wall and the use of creasing line patterns, which are examined more in detail only within the pressmolding process so far.

This study aimed to provide deeper insights into the limitations of the deep drawing process with immediate compression. The maximum forming ratio at convex shapes is investigated using the adapted blank holder force trajectory introduced in Hauptmann *et al.* (2016) with a cylindrical and rectangular base shape to gain more detailed knowledge on limitations. Furthermore, rounding radii at the bottom of the shape and edge radii in the base shape were analyzed, and the effect of blank preparation, with the help of creasing line patterns, to support the forming process limitations is discussed.

bioresources.com

EXPERIMENTAL

Materials

Three material grades were used in the experimental investigations. As a reference, all experiments were conducted with a fresh fibre grade typically used in tray forming applications, Trayforma® Natura (material 1, supplied by Stora Enso, Imatra, Finland), with a grammage of 350 g/m². Furthermore, a laboratory board grade (material 2) made of northern bleached softwood kraft pulp and 10% of a two-component polyethylene terphthalate (PET) technical fibre, which was introduced by Hauptmann *et al.* (2015), was used to investigate the edge radii at rectangular base shapes in a grammage of 350 g/m². This board grade was engineered for improved fiber-to-fiber mobility during forming processes. A fresh fibre grade called Fibreform® (material 3, Billerud Korsnäs, Solna, Sweden), which was engineered for improved extensibility of over 12%, was used to investigate the bottom radius. This material was used in a grammage of 310 g/m² from two layers glued together with a polymer binder. The basic mechanical properties from tensile testing are presented in Table 1.

Table 1. Basic Tensile Properties of the Paperboard Grades

Material	Tensile strength [kN/m]		Strain at break [%]		Thickness [mm]
	MD	CD	MD	CD	
1	22.0	11.6	4.3	6.0	0.43
2	8.9	6.8	3.5	4.0	0.70
3	26.5	14.1	17.1	13.6	0.34
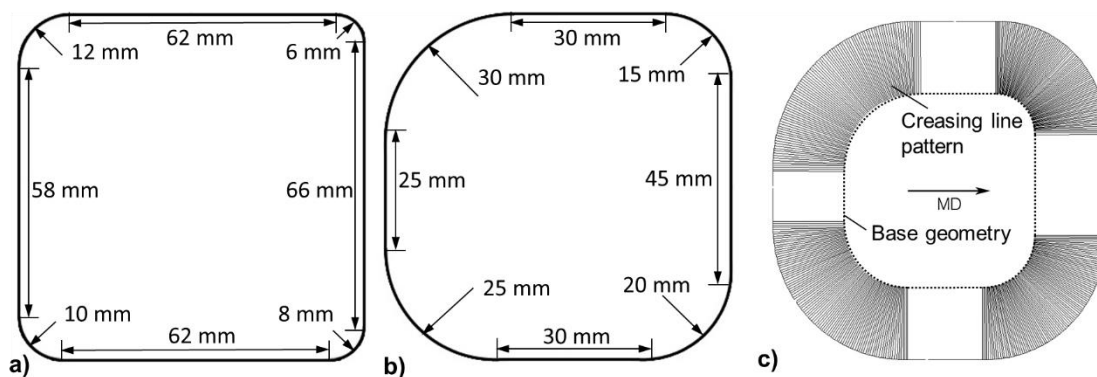
Fig. 1. a) Geometrical features of the base shape of the tool set 1, b) Geometrical features of the base shape of the tool set 2, c) Example of a creasing line pattern on the blank

Experimental Setup and Parameters

All experiments were conducted at the servo-hydraulic deep drawing press at TU Dresden, which was previously described (Hauptmann and Majschak 2011; Hauptmann and Majschak 2016). The press was placed in a room with standard climate of 23 °C and 50% humidity. The drawing speed was set to a constant value of 20 mm/s. Tool temperatures were varied between 80 and 220 °C for both punch and cavity, and the blank holder force was varied between 500 to 25,000 N to obtain the best forming results. The punch radius was 5 mm and 10 mm, with cylindrical tools having a diameter of 110 mm.

The experiments comparing punch radii were conducted with a drawing height of 25 mm, a clearance of 0.4 mm, and a 0.3° cone angle at the punch. To increase the forming ratio within the given space in the deep drawing press, a reduced base diameter of 77 mm was used with the same forming clearance and cone angle (0.4 mm, 0.3°). The forming height levels were increased in steps of 5 mm to a maximum of 65 mm nominal value.

The limitations originating from edge radii at rectangular base shapes were determined by 8 edge radius levels from 6 to 30 mm in combination with 4 drawing height levels from 10 to 40 mm, as a limitation through a certain edge radius leading to ruptures always must be seen in relation to the drawing height. The variation was realized by two tool sets with rectangular base shapes and each of the four different edge radii (Fig. 1a and b). This arrangement concurrently leads to differences in the straight length between the edge radii. In contrast to all other investigations, which have been focused on the occurrence of ruptures and determine basic limits thereby, the straight length levels were evaluated with respect to their influence on the springback angle of these sections in the base shape. The punch radius for the rectangular geometry and within increasing forming ratio was 0.5 mm and the cavity radius at the infeed was 3 mm in all experiments. Table 2 summarizes all parameters used in this part of the study.

Table 2. Geometrical Parameters of the Rectangular Tools with Rounded Edges

| Tool Sets	Edge Radius (mm)	Straight Length between Radii (mm)	Width x Length (mm)	Drawing Clearance/ Cone Angle (mm/°)	Wall Height (mm)
1	6	66	80 x 80	0.4/0.3	10
	8	62			20
	10	58			30
	12				40
2	15	45	80 x 80	0.4/0.3	
	20	35			
	25	25			
	30				

The blanks were prepared as concentric offset geometries of the base geometry (Fig. 1c). The offset corresponds to the nominal drawing height. Additionally, some of the blanks used for the forming experiments were prepared with a creasing line pattern. A creasing knife with a thickness of 0.7 mm was used. The counterpart was a compressible felt, and the preparation was conducted on a standard 2D-cutter (Zünd M-1200). The creasing lines were oriented radial to the middle point of the edge radii with an angular partition of 1° (Fig. 1c). Three further creasing lines were added at the transition to straight sections.

## RESULTS AND DISCUSSION

Influence of Punch Radius

Deep drawing of paperboard with immediate compression in the clearance between punch and cavity has typically been conducted with a sharp edge (radius 0.2 mm) at the punch in most of the recent publications. While such a small punch radius might lead to a higher material load in a narrow zone of the radius, this value was chosen to generate the

lowest backspring of the wall of 3D-shapes. The increase of the punch radius (bottom to wall radius at the 3D-shape) with material 1 led to the appearance of non-compressed wrinkles (Fig. 2a).
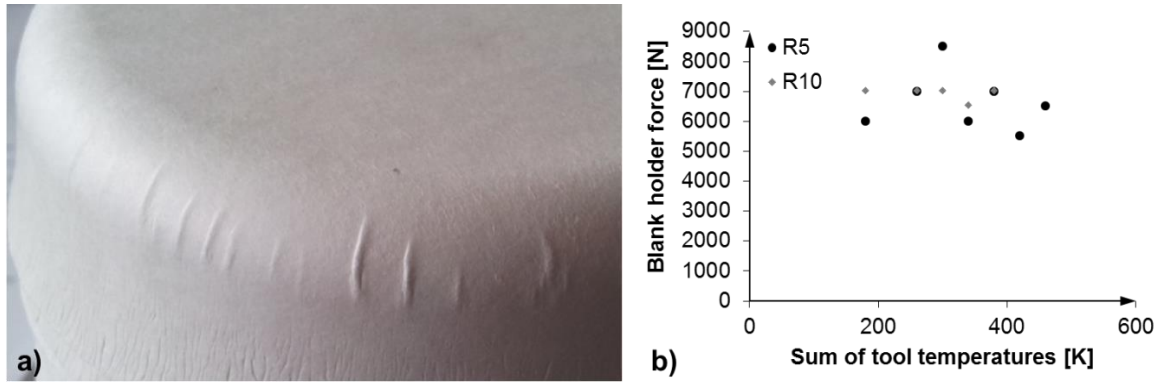

Fig. 2. a) Sample from material 1 with 110 mm base diameter, 25 mm wall height and a bottom radius of 10 mm showing non-compressed wrinkles at the radius; b) blank holder forces at different temperatures with 5 and 10 mm punch (bottom) radius (material 1)

The forming parameters were not affected by the increased punch radius. The maximum blank holder force applied ranged from 6,000 to 9,000 N and did not change noticeably if the punch radius was increased from 5 to 10 mm (Fig. 2b). The blank holder force for the 0.2 mm punch radius was reported to be 8,000 to 9,000 N (Hauptmann *et al.* (2015). Thus, the quality of the wrinkle distribution was not reduced at the wall, but it also did not improve with a higher punch radius. The wrinkles at the bottom radius were effectively reduced by an increased blank holder force (Fig. 3a). The wrinkles at the 5 mm radius were eliminated with the maximum blank holder force at elevated temperatures. The tool temperatures expressed by their sum represent the thermal energy intake as long as the drawing speed was kept constant. This thermal energy intake also had noticeable effects on the appearance of non-compressed wrinkles at the bottom radius. Increased thermal energy reduced the number of wrinkles (Fig. 3b).
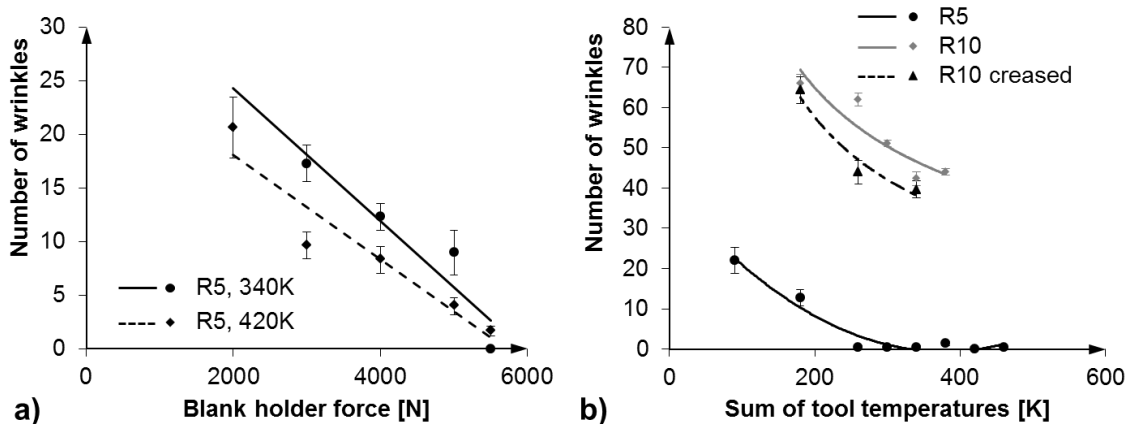
Fig. 3. a) Number of wrinkles at the bottom radius of 3D-shapes (110 mm base diameter, 25 mm height) plotted against the blank holder force for a sum of tool temperatures of 340 and 420 K; b) number of wrinkles in dependence of the sum of tool temperatures for 5 and 10 mm punch radius and 10 mm radius with a blank, which was prepared with a creasing line pattern (Fig. 1c)

For a radius of 5 mm and a sum of tool temperatures of 260 K, the wrinkles at the bottom fully disappeared using the maximum blank holder force, which was endured without ruptures by material 1 (Fig. 4a and b). The disappearance of wrinkles at the bottom coincided with an improved quality of the wall. With a 10 mm bottom radius, the wrinkles could not be avoided completely. However, there were a reduced number of wrinkles with increasing thermal energy, which was comparable to the effect of increasing blank holder force but not continuous in the case of thermal energy. After reaching 300 K, the number of wrinkles remained constant level, and further energy intake did not show any further effect. A preparation with a creasing line pattern had only minor effects on the appearance of wrinkles (Fig. 3b).
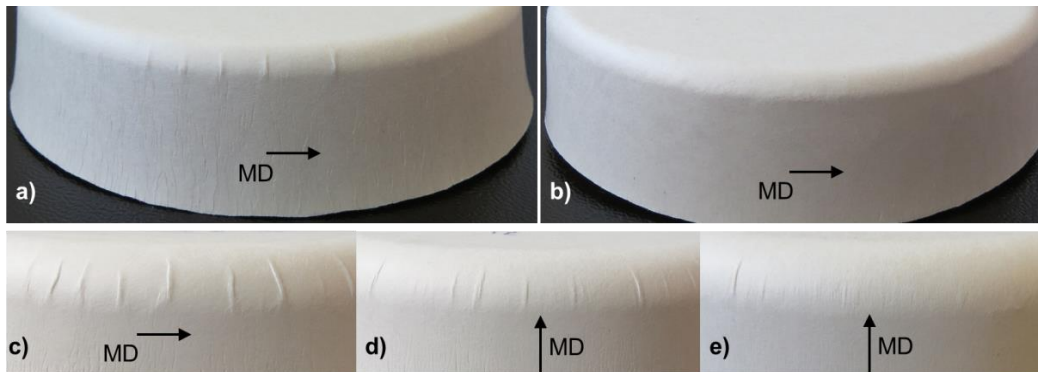
Fig. 4. a) Sample with 5 mm bottom radius showing wrinkles at the bottom radius (drawn at 2,000 N with 420 K from a blank of 160 mm diameter); b) sample with 5 mm bottom radius without wrinkles (drawn at 8,000 N and 320 K; c) wrinkles at the bottom radius of 10 mm of a sample after a) with compression in MD (drawn at 5,000 N and 300 K); d) wrinkles at the bottom radius of 10 mm of a sample after c) with compression in CD; e) wrinkles at the bottom radius of 10 mm of a sample after a) drawn at 8,000 N and 300 K

The wrinkling depended on the fiber orientation in the material. If the material was compressed in machine direction (MD), the wrinkles appeared more rough and clearly visible (Fig. 4c). Increased blank holder force and thermal energy first reduced or eliminated the wrinkles where compression was generated in cross direction (CD) (Fig. 4d and e), and the wrinkles appearing with compression in MD could not be eliminated and were more difficult to eliminate within the 5 mm radius.

A more extensible material (material 3) also showed wrinkles in the bottom radius over a wide range of parameter settings, but with optimized parameters the 10 mm radius could be formed without wrinkles (Fig. 5a). A material designed for improved compression behavior (material 2 with reduced strength, increased porosity) also prevented wrinkles within a 10 mm radius during deep drawing (Fig. 5b). It is likely that the mechanisms enabling the wrinkle-free forming of this bottom radius differed from each other. The more extensible material 3 was stretched near to its maximum at the beginning of the drawing process and prevented an excessive compression in plane during the first 10 mm of the punch motion. The more compressive material 2 in comparison did not provide high enough extensibility to form out the radius only from the tensile strain in the punch direction. It was more likely that the required compressive deformation was successfully compensated by its compressive strain through an increase in the initial height of wrinkles (Hauptmann *et al.* 2015).
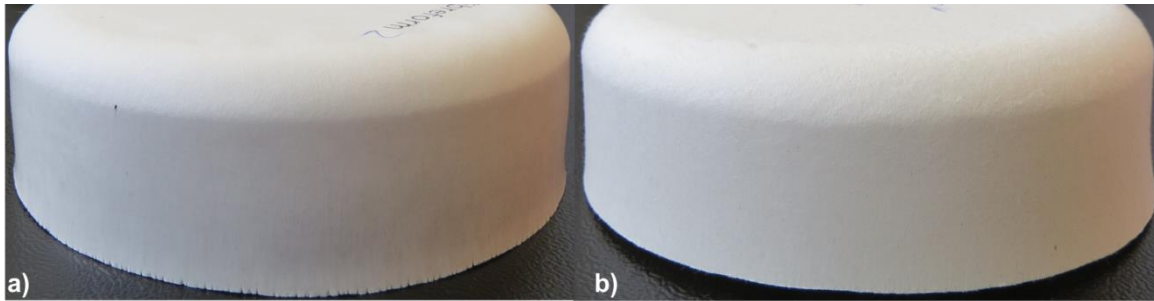
Fig. 5. a) Sample with 10 mm bottom radius from material 3 (8000 N, 340 K); b) sample with 10 mm bottom radius from material 2 (9000 N, 340 K)
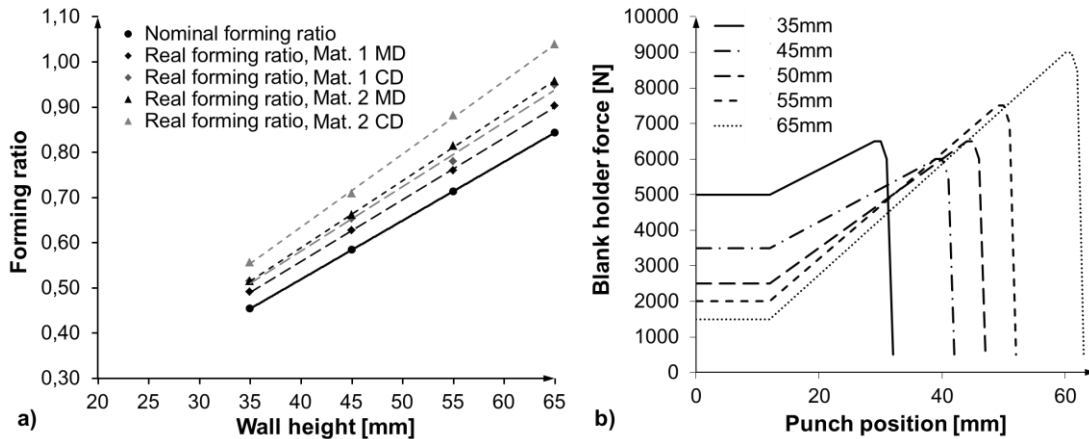
Limits of the Forming Ratio

Investigations of the forming ratio were varied on nominal levels with a drawing height of 35 mm (blank size of 147 mm diameter consisting of 2x35 mm+77 mm) to 65 mm at 77 mm base diameter, covering a range of 0.45 to 0.84. All of these nominal forming heights were successful and delivered rupture-free 3D-shapes for both material 1 (Fig. 6a) and material 2 (Fig. 6b) with a linear increasing blank holder force trajectory (Hauptmann *et al.* 2016).
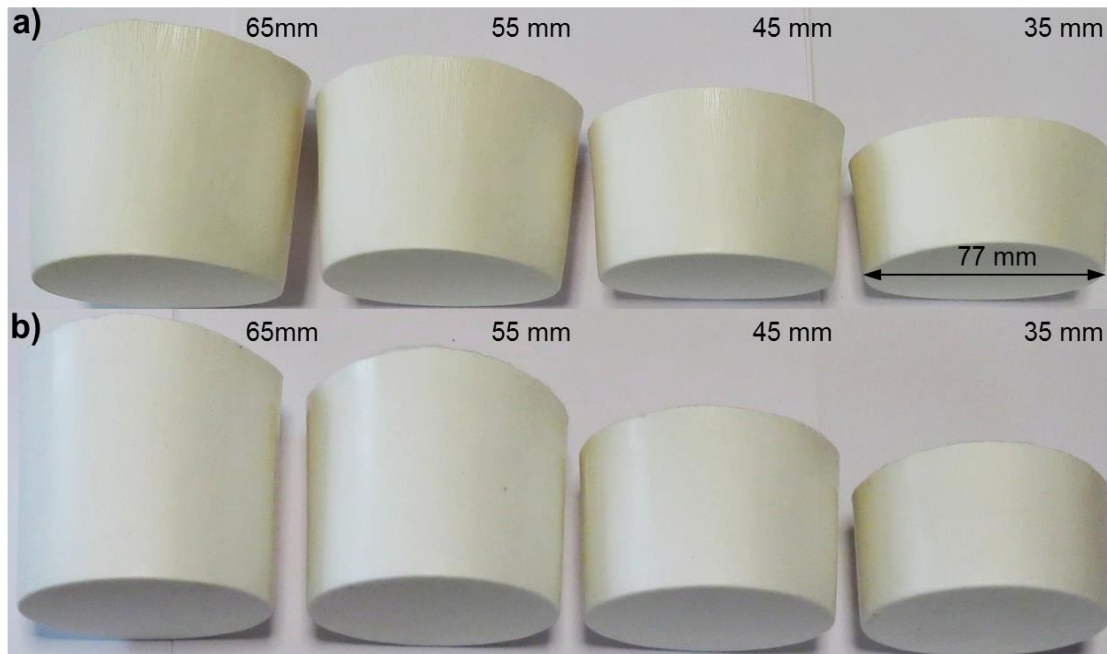
Fig. 6. a) Samples with different height levels made of material 1; b) samples with different height levels made of material 2

The strain of the wall was able to contribute crucially to the final height of the samples. To display this contribution, a real forming ratio was determined by the use of the real forming height measured at the wall of the samples, while the nominal forming ratio refers to the target height of 35 to 65 mm. Figure 7a shows the difference between nominal and real forming ratio for material 1 and 2 with strain in MD (black curves) and CD (gray

bioresources.com

curves). There was always a higher strain in CD than in MD. The strain along the wall of material 1 in MD ranged from 6 to 9%, and strain in CD was 9 to 13%. Material 2 provided 13 to 14% strain in MD and 21 to 23% in CD. The standard deviation of the measured wall heights was 1 to 4%. Both materials showed a basic tensile strain at break of 2 to 3% in MD and 4 to 6% in CD, which was clearly lower than the strain achieved at the wall of 3D shapes. These results were similar to those presented in Hauptmann *et al*. (2016). It can be assumed that the shear load at the wall inside the tools along the wall height under concurrent compressive load was the origin of elevated elongation at the wall.

Fig. 7. a) Theoretical and real forming ratio in dependence of the forming height for cylindrical base diameter of 77 mm; b) blank holder force trajectories applied with different nominal forming height
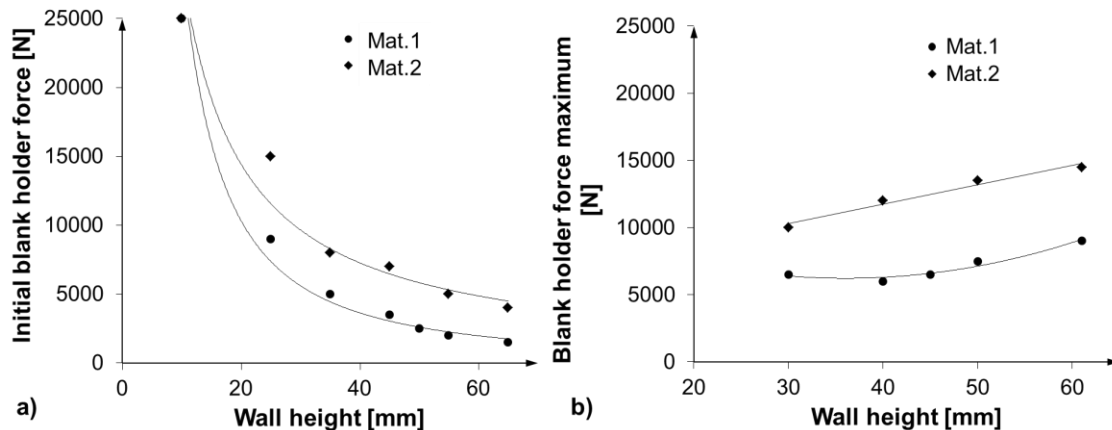

Fig. 8. a) Dependency of initial blank holder force from the wall height level for materials 1 and 2; b) blank holder force maximum in dependence of the wall height level for materials 1 and 2

The real forming ratio in MD thereafter was in a range of 0.49 to 0.9 for material 1 and 0.51 to 0.96 for material 2, while in CD the forming ratio exceeded the value 1 for material 2. With increasing forming ratio, the initial blank holder force at the beginning of the drawing process had to be reduced continuously (Fig. 7b) to avoid ruptures at the bottom. The necessary decrease of the blank holder force followed a power function (Fig. 8a). Within lower forming ratios the decrease needed to be more intensive than within higher forming ratios. This decrease is expected due to the proportional increasing material

bioresources.com

cross section creating resistance against compression in plane. This compressive resistance must be overcome in order to draw the material into the cavity and if so wrinkles appear. This increasing compressive resistance or resistance against wrinkling reduces the blank holder force because both forces in addition must be endured as tensile load at the bottom geometry which did not increase. However, it was still possible to increase the blank holder force after the full compression inside the clearance was reached beginning even from the lowest initial blank holder force (Fig. 7b). The force maximum also could be increased with higher forming heights due to the continuous increasing cross section resisting the tensile load after the material is under compression. The increase of the force maximum however showed only a moderate incline that was approximated with a linear or quadratic function (Fig. 8b).

The tendencies in the blank holder force were similar for both materials 1 and 2, but material 2 allowed higher blank holder forces and higher quality than material 1. The blank holder forces applied to material 1 with the highest forming ratio indicated that this material was near its maximum forming ratio even if it was not possible to further increase the forming ratio with the available equipment because the initial blank holder force had to be reduced to 1,500 N. A reduction in blank holder force below 1,000 N is likely to cause ruptures because the wrinkles cannot be distributed uniformly, such that local compression could lead to ruptures. Material 2 allowed an initial blank holder force of 4,000 N and thereby provided clearly higher potential for a further increase in forming ratio. In the cross direction, the material showed a real forming ratio above 1. Thus, it was assumed that a further increase in forming ratios in a range of 1.5 would be possible through adaptation of the blank holder force trajectory (Fig. 7b). The difference between the two materials with respect to the wrinkle distribution giving rise to such assumption is shown in Fig. 9. While the surface of material 1 (Fig. 9a) showed an uneven wrinkle distribution, especially near the bottom, the wrinkles were hardly visible at the surface of material 2 (Fig. 9b). The glossy surface proved a very even distribution of the material excess, which indicated further potential for increase in the forming ratio.
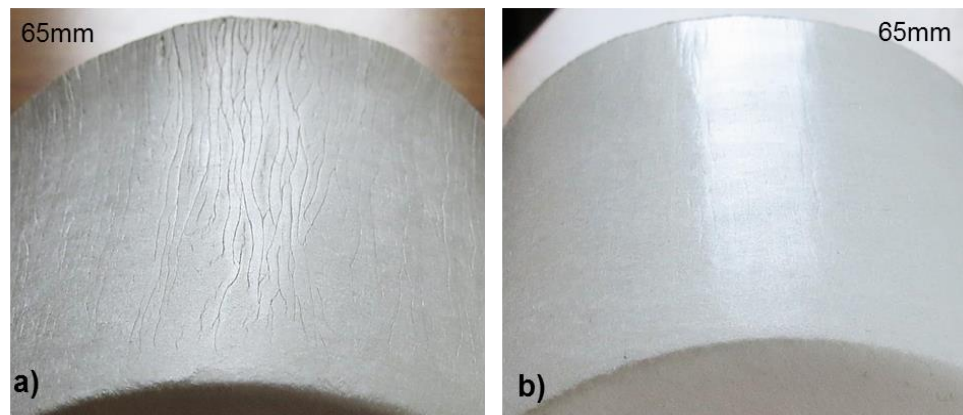

Fig. 9. a) The surface of a 3D-shape (77 mm diameter, 65 mm height) from material 1; b) the surface of a 3D-shape with size and height similar to material 2

## Limits of the Edge Radius at Rectangular Base Shape

The limitations described within the considerations to the forming ratio cannot be transferred directly to rectangular base shapes with rounded edges because the straight

sections in the base shape also endure tensile load. It was assumed that a higher forming ratio could be achieved at the edge radii. The results of forming tests using material 1 with edge radius levels 6 to 30 mm and wall height levels 10 to 40 mm showed that all radii could be formed successfully within a forming height of 10 mm. First, ruptures appeared at a 20 mm wall height. The capability of forming one of the radius levels was evaluated by the maximum blank holder force that could be applied before a rupture appeared. The radius of 6 and 8 mm led to ruptures. From the 10 mm to the 30 mm radius, the blank holder force increased almost linearly (Fig. 10a). The force always decreased at the 12 and 30 mm radius. This effect demonstrated that these two radii were positioned beside the lowest radii of 6 mm at tool set 1 and 15 mm at tool set 2 (see also Fig. 1a and b), and it seemed that the smaller radii affected the higher ones. As expected, the blank holder forces were higher within lower wall heights. When a preparation of the blank through application of a dense pattern of creasing lines was included (Fig. 1c), the blank holder force was clearly increased (Fig. 10), and the 8 mm radius was formed successfully to a height 30 mm. Thus, creasing lines reduced the force needed to initiate the wrinkling and thereby allowed an extended range for the blank holder force. The blank holder force level was nearly in the same range with increasing forming height if creasing line pattern was applied the blank and a limit seemed to establish at 3,000 N within higher wall height and edge radius.
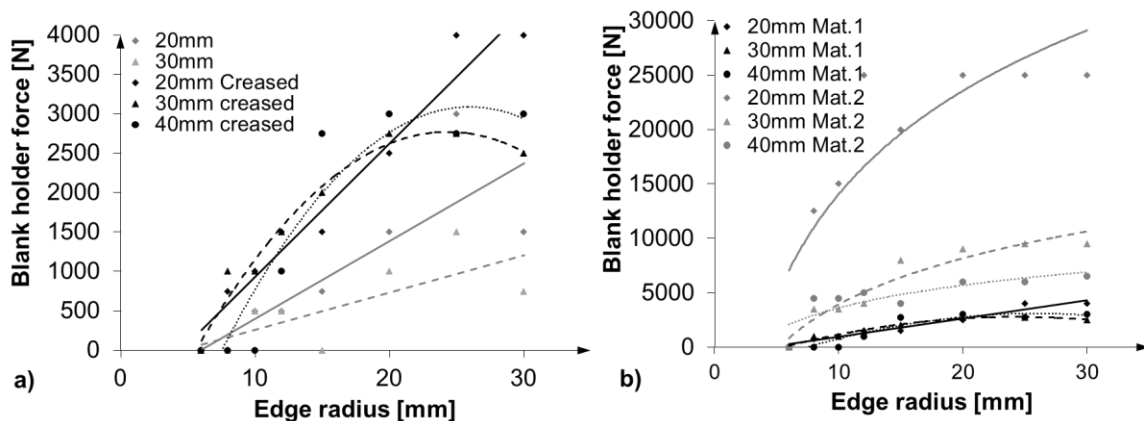
Fig. 10. a) Blank holder force in dependence of the edge radius of the base shape for various drawing height levels (solid: 20 mm, dashed line: 30 mm, dotted line: 40 mm) with and without creasing line pattern at the blanks; b) blank holder force in dependence of the edge radius for various drawing heights with blanks prepared with creasing line pattern for material 1 and 2 in comparison

Material 2 again allowed higher blank holder forces than material 1, especially at the 20 mm wall height (Fig. 10b). Within higher wall heights the difference was smaller, but still nearly double the blank holder force level could be applied. In these blank holder force ranges, there was a difference in the visual appearance of the formed edge radii (Fig. 11). In particular, the smaller radii of 8 to 12 mm in material 1 with higher wall heights showed that the local material excess at the border could hardly be managed in such a small region of the radius. This led to an increased tendency to relocate the material excess to the straight sections of the wall (Fig. 12, left).
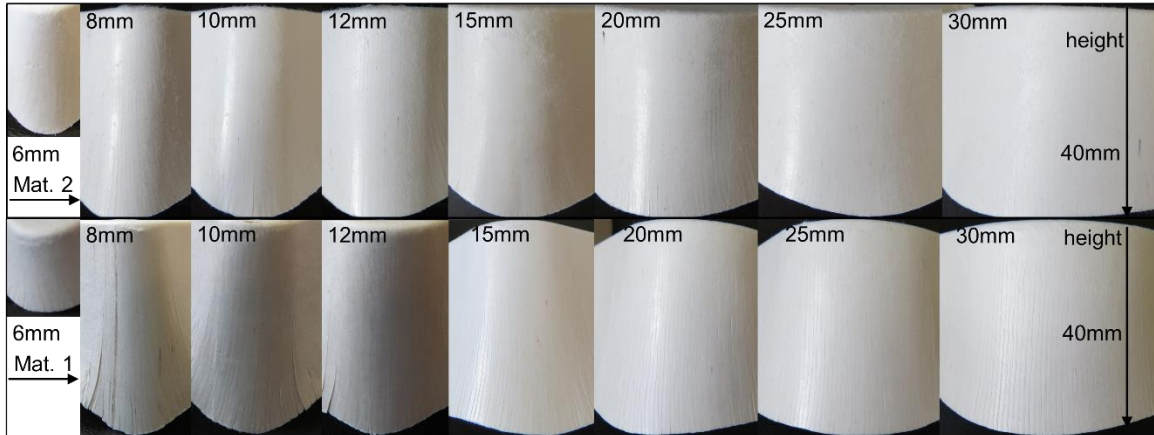
Fig. 11. Images of the edge radii with 40 mm wall height for radius 8 to 30 mm and a wall height of 20 mm for material 2 and 10 mm for material 1 at the maximum blank holder force for material 2 (upper row) and material 1 (row below) using creasing line pattern at the blank as support for wrinkling


Fig. 12. Samples of rectangular 3D-shapes made with the toolsets introduced in Fig. 1 from material 1 (left) with 15 mm radius in front and from material 2 (middle with radius 10 mm in front and right with radius 15 mm in front)

In material 2, the improved compressive strain and reduced resistance against wrinkling clearly reduced this tendency. Wrinkles in the straight section of the wall appeared only at the border between the smaller radii, where apparently material 2 also had reached its limits in compensating the material excess through compressive strain and uniform distribution of wrinkles (Fig. 12, middle and right). There was no wrinkle in the straight lines between higher radii formed with toolset 2. However the formation of wrinkles in the radii 15 to 30 mm was very uniform also with material 1. Hence, the visibility of the wrinkles in the straight sections could be considerably reduced by an adapted tool design that increases the compression in the straight sections. The tools were designed for the intensive increase in thickness at the radii, which did not appear in the straight section. Therefore, a reduced clearance could be envisaged in straight sections to reach a uniform compression. In this case, the additional load at the bottom in the straight sections needs to be taken into account. It is difficult to describe the support that the straight section provides to the edge radius sections against a rupture at the bottom. However, it is apparent that there is notable support because the isolated forming ratio at the edge radius of 10 mm for material 1 with a 30 mm wall height would be 1.5; for material 2, an edge

bioresources.com

radius of 8 mm with a wall height of 40 mm would lead to a forming ratio of 2.5. Both would be out of reach with basic cylindrical tools. If the assumption was that the full straight section supports the edge radius section, a modified forming ratio referring to the circumference of the base shape (instead of the diameter) should be more applicable and comparable. In this case, an edge radius of 8 mm at all four edges and the basic rectangular size of 80 mm would lead to a modified forming ratio of 0.13. This is half the value achieved by a 77 mm cylindrical base shape and a 65 mm wall height (0.27). These considerations suggest that only a certain part of the straight sections really supports the corresponding edge radius section.

It was expected that the straight sections of the rectangular shapes contribute significantly to the spring back. An isolated straight section would be formed by folding without material excess. This would suggest that with increasing length of the straight sections, the spring back also increases. This tendency was not recognized within the range of straight lengths used in this study, but instead, the spring-back angle was reduced with increasing straight length (Fig. 13a). The result could suggest that the length was not varied independently. The length only resulted from the radius variation, and the high length levels were positioned between the small edge radii of the shape. It could be assumed that smaller edge radii were able to fix the shape better due to the more intensive material excess in this small region. This theory was further supported by the reduced spring back angle, which appeared with increasing wall height of the shapes (Fig. 13b). This tendency was recognized for all straight length levels. It is also likely that the range of the length levels was not sufficient. Higher lengths are likely to increase the spring back due to the limited zone of influence the edge radii were able to provide to prevent the higher spring-back, which could be expected for straight sections. The considered range from 25 to 66 mm still seems to be widely influenced by the edge radii.
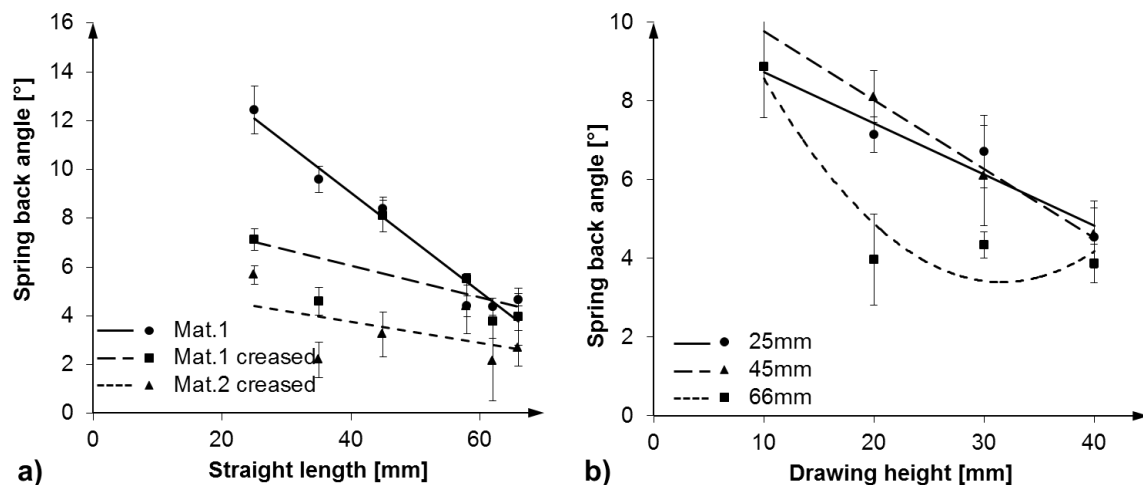
Fig. 13. a) Spring-back angle in dependence of the drawing height measured at different lengths of the straight section (straight length levels see also Fig.1a and b) for material 1; b) Spring-back angle in dependence of the length of straight sections for materials 1 and 2

CONCLUSIONS

1. The bottom radius represents a considerable failure potential at the beginning of the deep drawing process before the material comes into compression in the drawing clearance in terms of high local material load through sharp radius, which is especially critical with brittle materials such as groundwood pulp. An increasing bottom radius on the other hand leads to reduced quality through the appearance of non-compressed wrinkles. A starting point for such wrinkles must be expected at 5 mm radius for commercial board grade.

2. Increasing initial blank holder force and thermal energy intake reduces the non-compressed wrinkles at the bottom radius considerably. These wrinkles are reduced by rates of approximate one wrinkle each 200 N additional blank holder force and one wrinkle each 10 K additional tool temperature at commercial board grade (material 1). The increase of blank holder force and thermal energy is limited by the maximum load the material endures before ruptures at the bottom occur.

3. Improved extensibility and improved compressive deformation capacity of the board remarkably increases the radius at which non-compressed wrinkles occur. An improvement of extensibility by a factor 3 from an average of 5% (material 1) to an average value of 15% (material 3) enables the forming of a 10 mm radius instead of 5 mm without non-compressed wrinkles.

4. The forming ratio can be exploited by increasing the blank holder force. The initial blank holder force must be reduced with increasing forming ratio and is an indicator for the final limit of the forming ratio. In contrast, the force maximum can be increased with higher forming height.

5. The maximum forming ratio with cylindrical base shape for commercial board grade is 0.9 to 1, while for materials with improved compressive deformation, the real forming ratio already delivered a value above 1 and is likely to provide further potential for increases to approximately 1.3 to 1.5.

6. The forming ratio of rectangular shapes with rounded edges is not directly comparable to that of cylindrical base shape because the straight sections support the edge sections.

7. The reduction of the edge radius strongly affects the wall height that can be drawn without ruptures. An edge radius of 6 mm at 10 mm wall height or 8 mm at 30 mm wall height represents the limits for the radius/wall height combination with commercial deep drawing material. Material with improved compressive deformation reaches a wall height of 20 mm at 6 mm radius and a wall height of 40 mm at 8 mm edge radius.

8. A creasing line pattern radial to the edge radii supports the achievable wall height within small radii and increases the blank holder force that can be applied.

9. The spring back at rectangular shapes is reduced with increasing wall height and is influenced by the size of the edge radius. Smaller radii lead to better fixation of the final shape.

ACKNOWLEDGMENTS

REFERENCES CITED

Groche, P., and Huttel, D. (2016). "Paperboard forming - Specifics compared to sheet metal forming," *BioResources* 11(1), 1855-1867. DOI:10.15376/biores.11.1.1855-1867

Hauptmann, M., Ehlert, S., and Majschak, J. P. (2014). "The effect of concave base shape elements on the three dimensional forming process of advanced paperboard structures," *Packaging Technology and Science* 27(12), 975-986. DOI: 10.1002/pts.2089

Hauptmann, M., and Majschak, J. P. (2011). "New quality level of packaging components from paperboard through technology improvement in 3D forming," *Packaging Technology and Science* 24(7), 419-432. DOI: 10.1002/pts.941

Hauptmann, M., and Majschak, J. P. (2012). "Innovation aus Karton – Möglichkeiten der Formgestaltung von Verpackungskomponenten," in: *Proceedings of the 7th Fachtagung Verarbeitungsmaschinen und Verpackungstechnik (VVD)*, Dresden, Germany, pp. 449-460.

Hauptmann, M., and Majschak, J. P. (2016). "Characterization of influences on the wall stability of 2 deep drawn paperboard structures," *BioResources* 11(1), 2640-2654. DOI: 10.15376/biores.11.1.2640-2654

Hauptmann, M., Wallmeier, M., Erhard, K., Zelm, R., and Majschak J.-P. (2015). "The role of material composition, fiber properties and deformation mechanisms in the deep drawing of paperboard," *Cellulose* 22(5), 3377-3395.DOI:10.1007/s10570-015-0732-x

Hauptmann, M., Weyhe, J. and Majschak, J. P. (2016). "Optimisation of deep drawn paperboard structures by adaptation of the blank holder force trajectory," *Journal of Materials Processing and Technology* 232, 142-152. DOI: 10.1016/j.jmatprotec.2016.02.007.

Mozetic, L. (2008). *Design and Development of a Laboratory Equipment for Forming of Double-curved Paperboard Surfaces*, M.S. Thesis, Royal Institute of Technology, KTH Stockholm, Sweden.

Östlund, M., Borodulina, S., and Östlund S. (2011). "Influence of paperboard structure an processing conditions on forming of complex paperboard structures," *Packaging Technology and Science* 24(6), 331-341. DOI: 10.1002/pts.942

Tanninen, P., Leminen, V., Eskelinen, H., Lindell, H., and Varis, J. (2015). "Controlling the folding of the blank in paperboard tray press forming," *BioResources* 10(3), 5191-5202. DOI: 10.15376/biores.10.3.5191-5202

Vishtal, A., and Retulainen, E. (2014). "Improving the extensibility, wet web and dry strength of paper by addition of agar," *Nordic Pulp and Paper Research Journal* 29(3), 434-443. DOI: 10.3183/NPPRJ-2014-29-03-p434-443